Excess free energy: integral equations

Let us consider the equilibrium density profile $\rho(r)$ and a reference density profile $\rho_0(r)$ for the same system. Assume the linear parametrization

$$\rho_\lambda(r) = \rho_0(r) + \lambda[\rho(r) - \rho_0(r)] = \rho_0(r) + \lambda\Delta\rho(r) \qquad \lambda \in [0:1]$$

From the definition of $c^{(1)}$ and $c^{(2)}$ as functional derivative we can write

$$F_{ex}[\rho] = F_{ex}[\rho_0] - k_B T \int_0^1 d\lambda \int d^3r \;\; \Delta\rho(r) c^{(1)}(r;[\rho_\lambda])$$

$$c^{(1)}(r;[\rho]) = c^{(1)}(r;[\rho_0]) + \int_0^1 d\lambda \int d^3r' \;\; \Delta\rho(r') c^{(2)}(r,r';[\rho_\lambda])$$

Using the second in the first and noticing that we get

$$\int_0^1 dx \int_0^x dy \; g(y) = \int_0^1 dx \; (1-x) \; g(x) \quad \forall g(x)$$

$$\begin{aligned} F_{ex}[\rho] &= F_{ex}[\rho_0] - k_B T \int d^3r \;\; \Delta\rho(r) c^{(1)}(r;[\rho_0]) \\ &- k_B T \int_0^1 d\lambda (1-\lambda) \int d^3r \; d^3r' \; \Delta\rho(r) c^{(2)}(r,r';[\rho_\lambda]) \; \Delta\rho(r') \end{aligned}$$

For homogeneous systems with ideal gas reference state

$$c^{(1)}(\rho) = -\beta\mu_{ex} = \int_0^\rho d\rho' \int d^3r c^{(2)}(r,\rho')$$

$$\frac{\chi_T^{(0)}}{\chi_T} = \left(\frac{\partial\beta P}{\partial\rho}\right)_T = \rho\left(\frac{\partial\beta\mu}{\partial\rho}\right)_T = 1 - \rho\int d^3r \; c^{(2)}(r,\rho) = 1 - \rho \; \hat{c}^{(2)}(k=0)$$

The effective one-component system

Integral equations approach and inversion procedure:

remember that
$$F_{ex}[\rho] = F_{ex}[\rho_0] - k_BT \int d^3r \;\; \Delta\rho(r) c^{(1)}(r;[\rho_0])$$
$$- \;\; k_BT \int_0^1 d\lambda (1-\lambda) \int d^3r \; d^3r' \; \Delta\rho(r) c^{(2)}(r,r';[\rho_\lambda]) \; \Delta\rho(r')$$

and consider the uniform reference system $\rho_0(r)=\rho_0$: $c^{(1)}(r,\rho_0)=-\beta\mu_{ex}$
Add the ideal contribution and switch back to Ω_V

$$\Omega_V[\rho] = \Omega_0(\rho_0) \;\; + \;\; \int d^3r \; \rho(r)\Phi(r) + k_BT \int d^3r \left[\rho(r) log \frac{\rho(r)}{\rho_0} - \Delta\rho(r)\right]$$
$$- \;\; k_BT \int_0^1 d\lambda (1-\lambda) \int d^3r \; d^3r' \; \Delta\rho(r) c^{(2)}([\rho_\lambda], r, r') \Delta\rho(r')$$

Replacing $c^{(2)}([\rho_\lambda],r,r')$ by $c^{(2)}(r-r')$ of the uniform system, the equilibrium condition for the functional provides the HNC equation

$$\rho(r) = \rho_0 exp\left\{-\beta\Phi(r) + \int d^3r' c^{(2)}(r-r')\Delta\rho(r')\right\} \qquad \text{HNC}$$

The effective one-component system

Percus (1962): consider one particle in the system as a test particle

$$\phi(r) = v(r) \qquad \text{the inter-particle potential}$$
$$\rho(r) = \rho_0 g(r); \qquad \Delta\rho(r) = \rho_0 h(r) \qquad \text{of the uniform system}$$

HNC+OZ: $g(r) = exp\{-\beta v(r) + h(r) - c(r)\}$ HNC closure for homogeneous systems

Percus-Yevik (PY): $g(r) = e^{-\beta v(r)}\,[g(r) - c(r)]$ PY, very accurate for hard spheres

Ideal gas limit: $\lim_{\rho \to 0} g(r) = e^{-\beta v(r)}$

HNC and PY provide a link between the pair structure g(r) and the two-body potential v(r) in a uniform system, if supplemented by:

Theorem (Henderson, Phy. Letts. 49A, 197 (1974)): in a quantum or classical fluid with only pairwise interactions, and at fixed thermodynamic conditions, the pair potential v(r) that give rise to a given radial distribution function g(r) is unique, up to a constant.
In other words, if a potential exists which generate a given g(r), this potential is unique up to a constant.

$$g(r) \quad \Longleftrightarrow \quad v(r)$$

The effective one-component system

Inverse problem: from a measured g(r) to a two body effective interaction v(r)

Theoretical basis for Boltzmann inversion, HNC inversion and Modified-HNC inversion

HNC inversion: $\beta v(r) = -\log[g(r)] + h(r) - c(r) - \log[g(r)]$

In a one component system, the original pair potential is recovered if the inversion procedure is exact (or fully converged for the iterative solutions). (Reatto et al. Phys. Rev. A33, 3541 (1986))

In a multi component system, inversion of radial distribution functions $g_{\alpha\beta}(r)$ provides effective two-body potentials $v_{\alpha\beta}(r)$ between species α and β.

- effective potentials are state dependent.
- effective potentials are obtained at finite density, at variance with $\omega_2(r)$ of the diagrammatic expansion which considered only two particles (zero density limit).

In a two component system, the effective pair potential $v_{11}(r)$ obtained from the inversion procedure is a resummation of all n-body terms in the diagrammatic expansion of the free energy.
The two body term of the diagrammatic expansion is only the zero density limit of the effective pair potential

$$\phi_{11}(R_{ij}) + \omega_2(R_{ij}; z_2) = \lim_{\rho_1 \to 0} v_{11}^{eff}(R_{ij}; \rho_1, z_2)$$

Drawbacks:
- the knowledge of the relevant g(r) is needed. Only possible for not too extreme size ratios.
- computing thermodynamics with density dependent potentials is more cumbersome

Polymeric systems

Single chain conformations

Polymers are macromolecules build up by repeating chemical units (*monomers*) bonded together in various topologies.

Relevant length scales for very long chains:

- the *atomic* length scale relevant for the local chemistry of monomers
- the *Kuhn* or *persistence* length is an intermediate length scale at which the atomistic details are lost and a number of *chemical monomers* have been coarse-grained into a single *physical monomer.*
- the chain size is the macroscopic length over which the polymer spread in space : end-to-end distance or radius of gyration

Primitive polymer model:

Physical monomers resolution: a sequence of point particles connected in a fixed topology.

Interactions:

- bond interactions between adjacent monomers along the chain
- steric interaction between any pair of monomers

particle positions	$r_i \qquad i \in [0, N]$
chain center of mass	$R_{CM} = \frac{1}{N+1} \sum_{i=0}^{N} r_i$
position relative to CM	$s_i = r_i - R_{CM} \qquad i \in [0, N]$
bond vectors	$\ell_i = r_{i+1} - r_i$
end-to-end vector	$R = r_N - r_0 = \sum_{i=1}^{N} \ell_i$
gyration radius	$R_g^2 = \frac{1}{N+1} \sum_{i=0}^{N} s_i^2 = \frac{1}{2(N+1)^2} \sum_{i,j} \lvert r_{ij} \rvert^2$

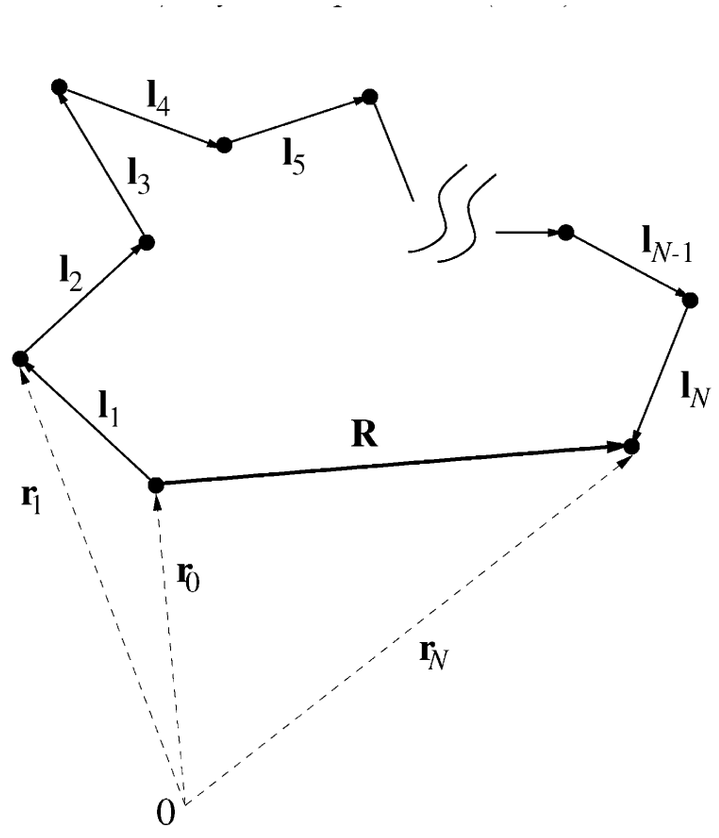

Single chain

For very large N (N$^{\rightarrow\infty}$), chains are self-similar objects, meaning that the property of part of the chain are identical to the property of the entire chain under a proper rescaling of lengths.
The physics of chains is expressed in terms of scaling laws

end-to-end distance $R =< R^2 >^{1/2} \sim N^{\nu}$
CM diffusion coefficient $D \sim N^{-\nu'}$

Ideal chain model:
• bonds of fixed length **a** or with gaussian distribution of length around **a**
• steric interaction is absent

$$R = a\sqrt{N} \longrightarrow \boxed{\nu_{id} = 0.5}$$

By central limit theorem: $W_0(R) \propto R^2 \exp\left(-\frac{3R^2}{2Na^2}\right).$

$$F_{\mathrm{el}}(R) = F(0) + \frac{3k_{\mathrm{B}}T}{2}\frac{R^2}{Na^2}\,,$$ Elastic free energy of an ideal chain

Self avoiding walk model (SAW):
• bonds of fixed length **a** or with gaussian distribution of length around **a**
• steric monomer-monomer interaction: $v_{\mathrm{mm}}(\boldsymbol{r}_n, \boldsymbol{r}_m) = v_0 k_{\mathrm{B}} T \delta(\boldsymbol{r}_n - \boldsymbol{r}_m)\,,$

Single chain

Flory's mean field argument for SAW:
the number of monomer that can fit into a volume R^3 without overlap is R^3/v_0. The probability that one segment will not overlap with another is $(1-v_0/R^3)$. For $N(N+1)/2$ distinct pairs we have

$$P_{int}(R) \propto \left(1-\frac{v_0}{R^3}\right)^{N(N+1)/2} = \exp\left[\frac{N(N+1)}{2}\log(1-v_0/R^3)\right] \simeq \exp\left\{-\frac{N^2 v_0}{2R^3}\right\}$$

Free energy: $$\beta F_{tot} = \beta F_{el} + \beta F_{int} = \frac{3R^2}{2Na^2} + \frac{N^2 v_0}{2R^3}$$

equilibrium state (minimum): $$R^5 = v_0 a^2 N^3 \rightarrow R \sim N^{3/5} \quad \Longrightarrow \boxed{\nu_{saw} = \frac{3}{5} = 0.6}$$

At d dimensions: $$\nu_{saw} = \frac{3}{d+2} \quad \rightarrow \nu_{saw} = \frac{1}{2} \quad \text{for} \quad d = 4$$

At d=4, the excluded volume is negligeble.
Renormalization Group study at d=4 and (4-ε) expansion provides: $\nu_{saw} = 0.588$
in agreement with MC simulations and close to Flory's value.

Single chain: effect of the solvent

Lattice model of a chain in solvent

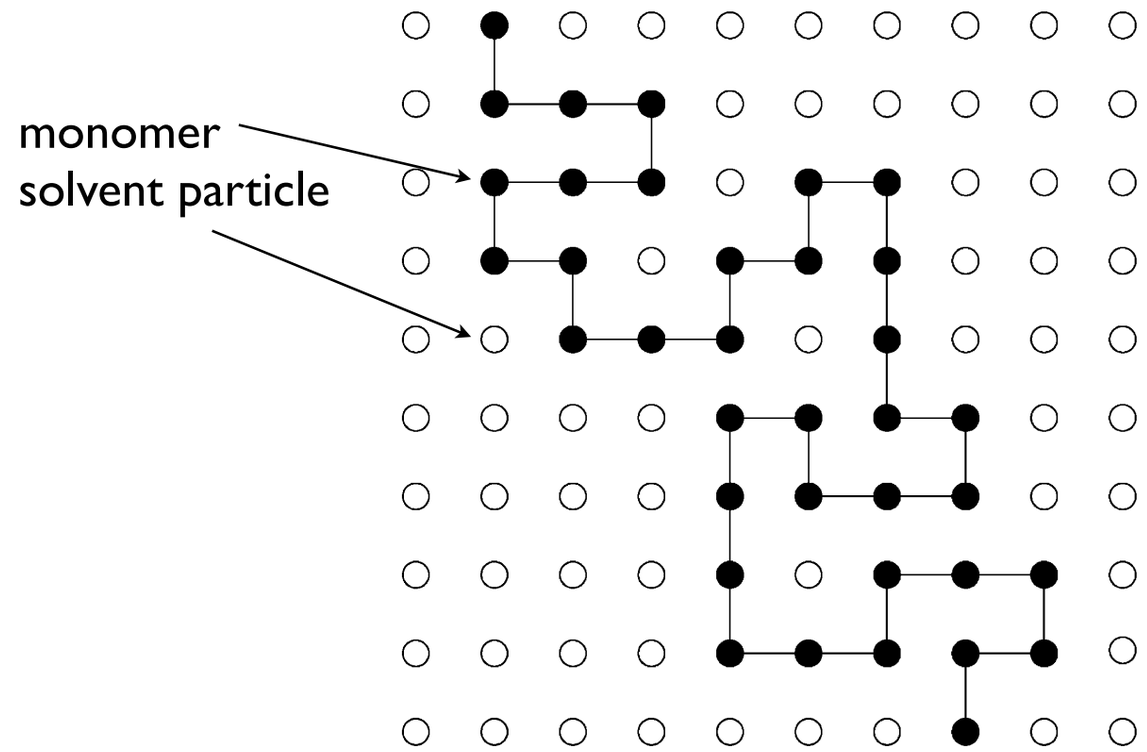

nearest-neighbors attractions:

monomomer-monomer	$-\epsilon_{pp}N_{pp}$
monomer-solvent	$-\epsilon_{ps}N_{ps}$
solvent-solvent	$-\epsilon_{ss}N_{ss}$

Average energy from these interactions:

$$E = -\epsilon_{pp}N_{pp} - \epsilon_{ps}N_{ps} - \epsilon_{ss}N_{ss}$$

- N_{pp}=average number of pp contacts
- N_{ps}=average number of ps contacts
- N_{ss}=average number of ss contacts

Monomers uniformely distributed inside R^3: $\phi_p = v_0 N/R^3$

$$N_{pp} = \frac{1}{2} z N \phi_p$$
$$N_{ps} = zN(1-\phi_p)$$
$$N_{ss} = \frac{N_s(N_s-1)}{2} - N_{pp} - N_{ps}$$

$$\beta E(R) = -\frac{N^2 v_0}{R^3}\chi; \qquad \chi = \frac{\beta z}{2}(\epsilon_{pp} + \epsilon_{ss} - 2\epsilon_{ps})$$

Free energy: $$\beta F_{tot} = \beta F_{el} + \beta F_{int} = \frac{3R^2}{2Na^2} + \frac{N^2 v}{2R^3}; \qquad v = v_0(1-2\chi)$$

Single chain: effect of the solvent

three distinct regimes

a) *good solvent* conditions: $(1-2\chi)>0$ high T $\nu>0$ and $\nu=3/5$

b) *poor solvent* conditions: $(1-2\chi)<0$ low T $\nu<0$ and $\nu=1/3$

c) θ-*solvent* condition: $(1-2\chi)=0$ $T=T_\theta$ $\nu=0$ and $\nu=1/2$

in crossing T_θ the chain undergoes a coil-to-globule transition. For very large N this is a dramatic change in size (phase transition).

Polymer solutions

System of M chains of the same length N in a solvent in a volume V.
The relevant thermodynamics variable is the chain density $\rho=M/V$,
$\rho^*=3/(4\pi R^3)$= chain overlapping density $\sim N^{-3\nu}$
In good solvent we can distinguish three regimes

a) *Dilute solutions*: $\rho/\rho^*<1$ large monomer fluctuations
b) *Semidilute regime*: $\rho/\rho^*>1$ large monomer fluctuations
c) *Concentrated regime*: $N\rho \sim 1$ small monomer fluctuations

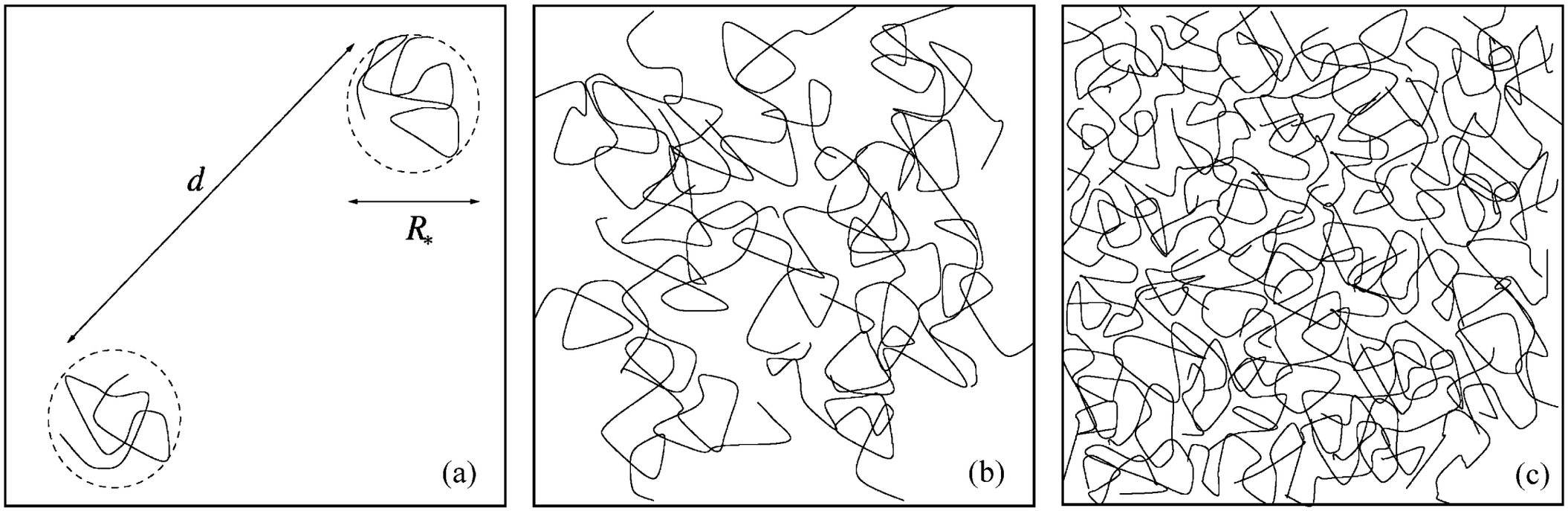

Fig. 11. The three concentration regimes for polymer solutions: (a) dilute, where the average separation d between the coils is much larger than the typical size R_* of the coil; (b) semidilute, above the overlap concentration c_*; (c) concentrated solution, above the concentration c_{**}.

c^*=monomer concentration at overlap: $c^*=N\rho^* \sim N^{1-3\nu} \ll 1$ for large N ($N^{-4/5}$ in GS)
extremely low monomer densities for semidilute solution of large chains

Polymer solutions

Flory-Huggins: mean field theory of the solution provide qualitively correct phase behaviour which become quantitative at high concentrations (negligible fluctuations)

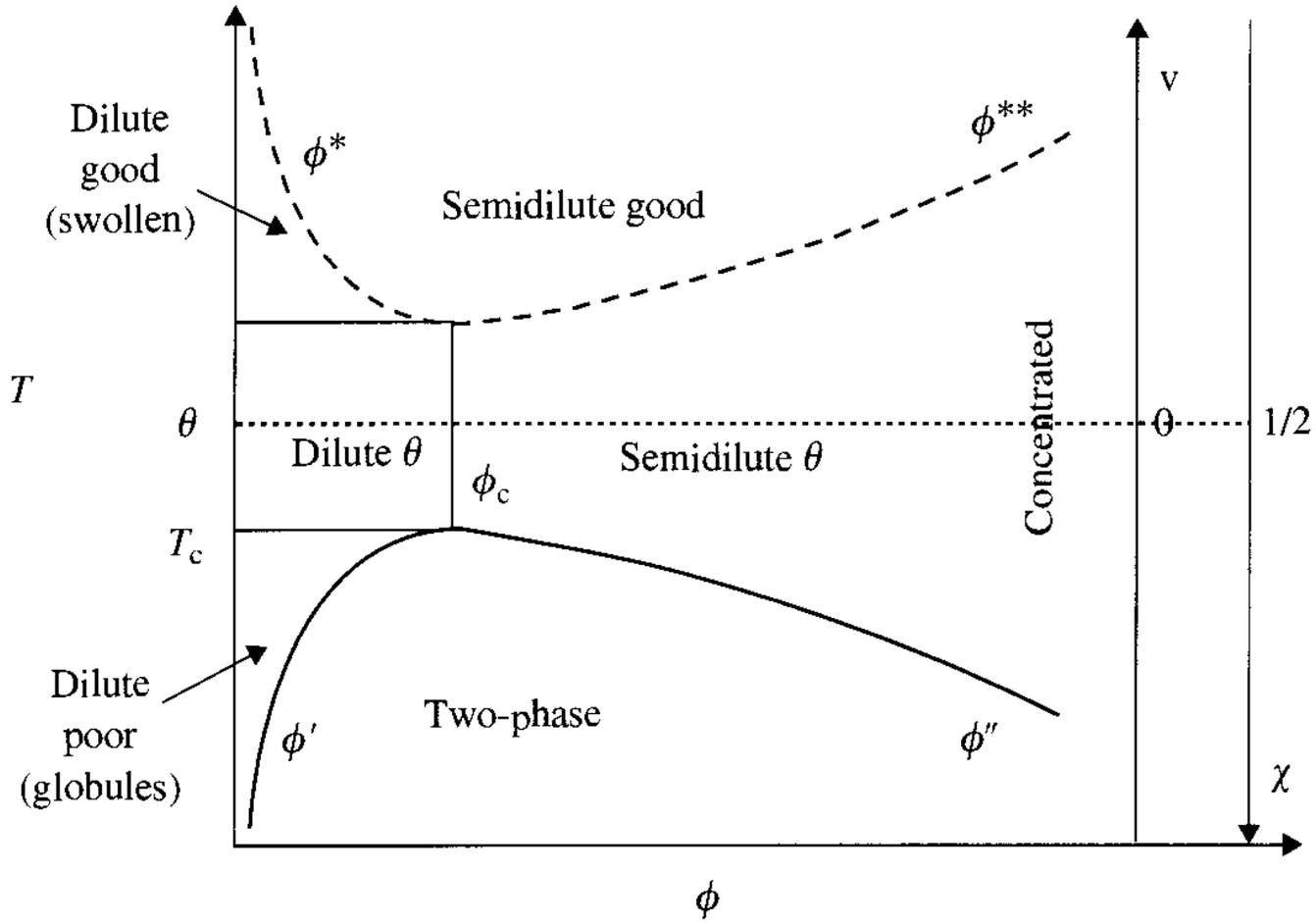

Fig. 5.1
Phase diagram for polymer solutions with a UCST. The solid curve denotes the binodal and phase separation occurs for polymer solutions with T and ϕ below the binodal. The dashed curve is the low temperature boundary of the semidilute good solvent regime.

Polymer solutions

Scaling theory: chains are self-similar, the physics is unchanged if one groups λ monomers together and rescale the distances

$$N \to \lambda^{-1} N \qquad \text{and} \qquad a \to \lambda^{\nu} a$$

Osmotic pressure: $\Pi = c k_B T f(a^3 c, N)$ f is dimensionless

$$c \to \lambda^{-1} c \qquad \Longrightarrow f(a^3 c, N) = \lambda^{-1} f(\lambda^{3\nu-1} a^3 c, \lambda^{-1} N) = \frac{1}{N} \hat{f}(a^3 c N^{3\nu-1})$$

In terms of the overlap monomer concentration $c^* = a^{-3} N^{1-3\nu}$

$$\boxed{\Pi(c) = \frac{c k_B T}{N} \hat{f}\left(\frac{c}{c^*}\right)}$$

- in the dilute regime van't Hoff's law implies $\lim_{x \to 0} \hat{f}(x) = 1$

- in the semidilute regime Π must become independent on N: $\hat{f}(x) \sim x^{\alpha} \qquad \alpha = \frac{1}{(3\nu - 1)}$

$$\boxed{\Pi(c) \sim \frac{c k_B T}{N} \left(\frac{c}{c^*}\right)^{1/(3\nu-1)} \sim c^{9/4} \qquad \text{good solvent}}$$

Confirmed by experiments and at variance with the c^2 behaviour predicted by mean field theory.

Polymer solutions

Chain size in good solvent:

dilute regime: $\nu=3/5$ excluded volume statistics at all lengths scale

concentrated regime: $\nu=3/5$ at intermediate length scales below the screening length ξ

$\nu=1/2$ at larger length scale

$R\sim\xi^{1-1/2\nu} N^{1/2}$ ideal chain statistics

semidilute regime from scaling: $$R(c) = R(0)\tilde{f}\left(\frac{c}{c^*}\right) = aN^{\nu}\tilde{f}\left(\frac{c}{c^*}\right)$$

$$c << c^* \qquad \tilde{f}(x) = 1$$

$$c >> c^* \qquad R(c) \sim aN^{\nu}\left(\frac{c}{c^*}\right)^{\delta} \sim N^{1/2}$$

$$c^* = a^{-3}N^{1-3\nu} \qquad \rightarrow \qquad \delta = \frac{1-2\nu}{6\nu-2} = -\frac{1}{8} \qquad (\nu = 3/5)$$

$$\begin{aligned} R(c) &\sim aN^{\nu}\left(\frac{c}{c^*}\right)^{\frac{1-2\nu}{6\nu-2}} \sim c^{-\frac{1}{8}} \\ \xi &\sim c^{-\frac{3}{4}} \end{aligned}$$

in agreement with experiments

Coarse-grained model for polymer solutions

• Implicit solvent model of polymer solutions: solvent effects is already represented through an effective monomer-monomer interaction (nearest-neighbor if on lattice).
• reduce each chain to its center of mass by averaging over all monomer degrees of freedom

• for very long realistic chains (N~1000) this is enormous reduction in the number of degrees of freedom: M chains of N monomers ⟹ M soft particles

remark: since $c^* \sim N^{-4/5}$ very long chains are needed to have a large semidilute regime

• simulation of very long chains is notoriously very difficult because of the very long relaxation times involved.
• simulation of the effective model is trivial because the resulting effective potential is very soft.
• structural features of the chains are lost but thermodynamic behaviour is preserved

• how to compute the effective polymer-polymer interaction?

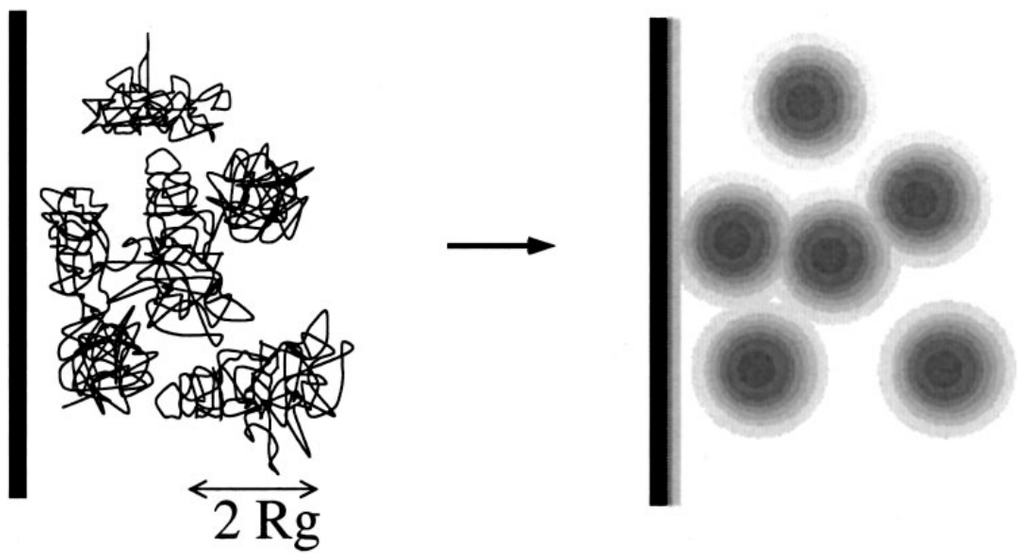

Can Polymer Coils Be Modeled as "Soft Colloids"?

A. A. Louis,[1] P. G. Bolhuis,[1] J. P. Hansen,[1] and E. J. Meijer[2]

Zero density limit: interaction potential between two isolated chains.
In this limit the potential is

$$\beta v_{pp}(R_1 - R_2) = -\log\left[g_{pp}(R_1 - R_2)\right]$$

$g_{pp}(R)$ is the pair distribution function of the two centres of mass at distance R.

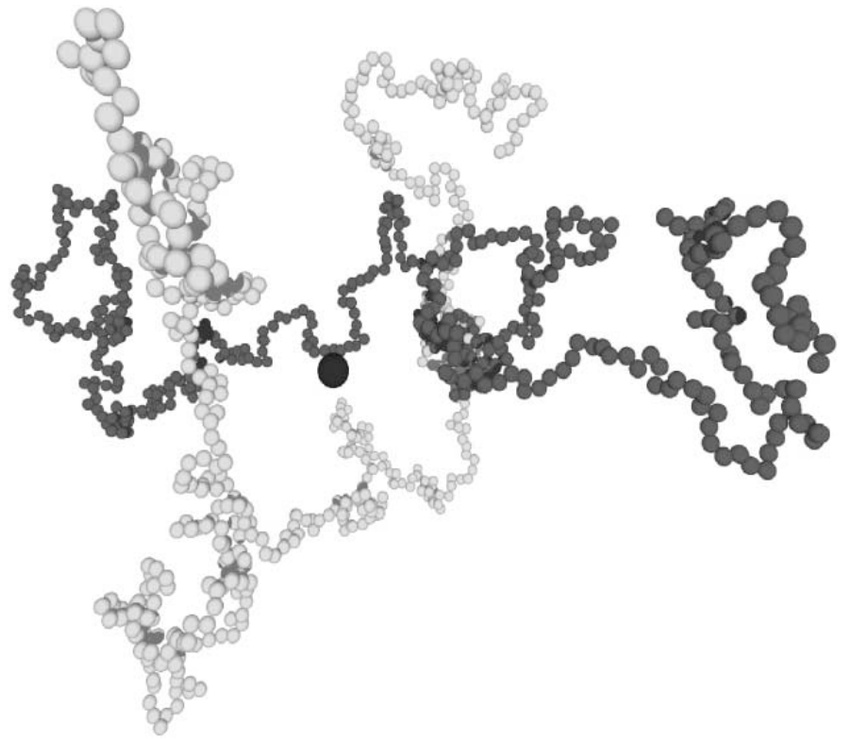

RGT provides a *universal* Gaussian Core Potential:

$$\frac{v(r)}{k_B T} \simeq A \exp[-\alpha(r/R_g)^2],$$

From MC calculations for N>100:

$$\begin{aligned} A(N) &= A_\infty + \frac{a}{N^\sigma} \qquad A_\infty = 1.75; a = 1.5; \sigma = 0.33 \\ \alpha &= 0.80 \\ R_g &= \text{chain radius of gyration} \end{aligned}$$

Coarse-grained model for polymer solutions

Finite density: HNC inversion is very accurate because of the softness of the potential

$$\beta v(r;\rho) = -\log[g(r)] + h(r) - c(r)$$

Remarks:

- the pair correlation decreases with increasing density (like for quantum particles) confirming that in the melt regime, polymers are uncorrelated.
- the effective interaction at zero distance is always ~2kT and has a non monotonous behaviour with ρ
- the effective potential is only moderately density dependent and is well fitted by a sum of gaussians
- the effective range of the interaction tends to increase with ρ, and the potential develops a small amplitude negative tail for $r>>R_g$

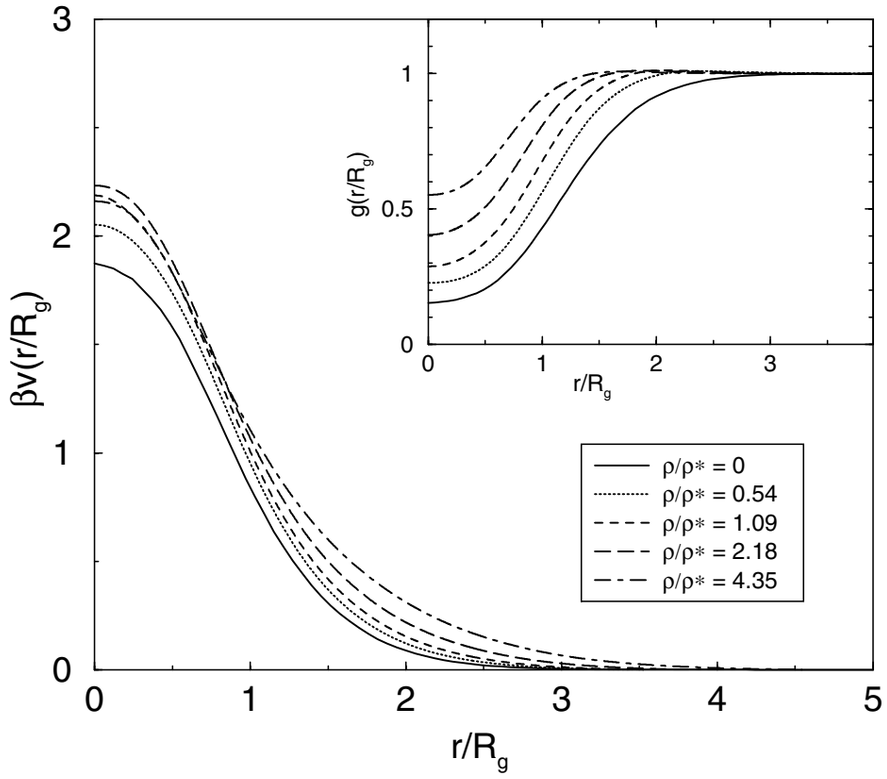

FIG. 1. The effective polymer CM pair potential $\beta v(r/R_g)$ derived from an HNC inversion of $g(r/R_g)$ for different densities. The x axis denotes r/R_g, where R_g is the radius of gyration of an isolated SAW polymer. Inset: The polymer CM pair distribution function $g(r)$ calculated for $L = 500$ SAW polymers and used to generate $\beta v(r)$.

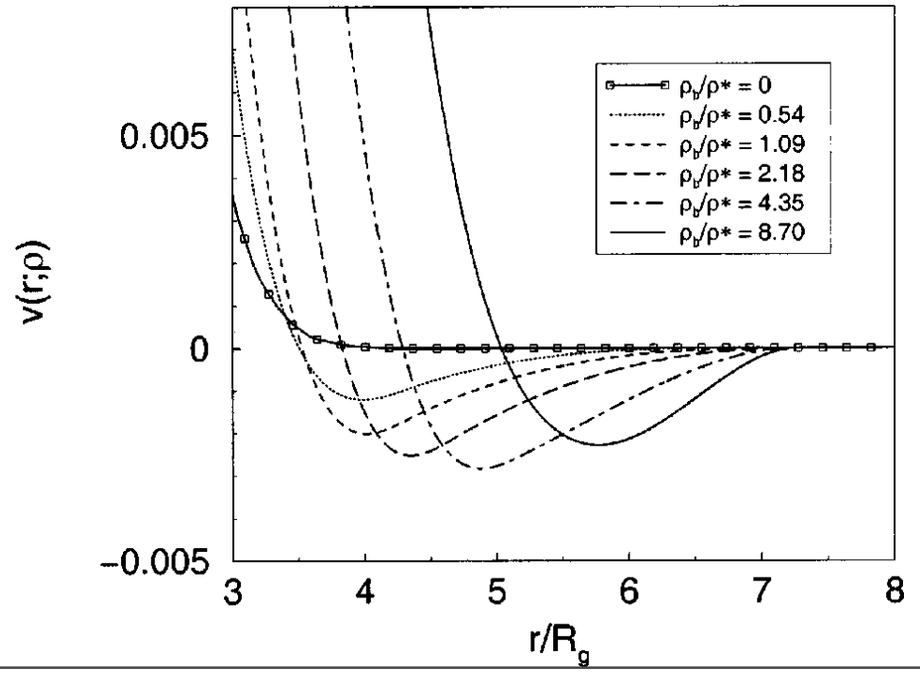

Link with thermodynamics via the compressibility relation

$$\beta P(\rho) = \int_0^{\rho} [1 - \rho' \hat{c}(k = 0; \rho')] \, \mathrm{d}\rho'$$

Remarks:

• it is well known (Stillinger) that the 'gaussian core model' has an EOS quadratic in density which violates scaling

$$\beta P = \rho + \tfrac{1}{2} \beta \hat{v}_2(k = 0) \rho^2.$$

• incorporating the density dependence into the potential restore the correct des Cloizeaux scaling $\rho^{9/4}$

• the inversion procedure does not provide the volume term necessary to compute the free energy of the effective model. However the observed agreement between OES for the full monomer and the effective polymers suggests that this term is negligibly small

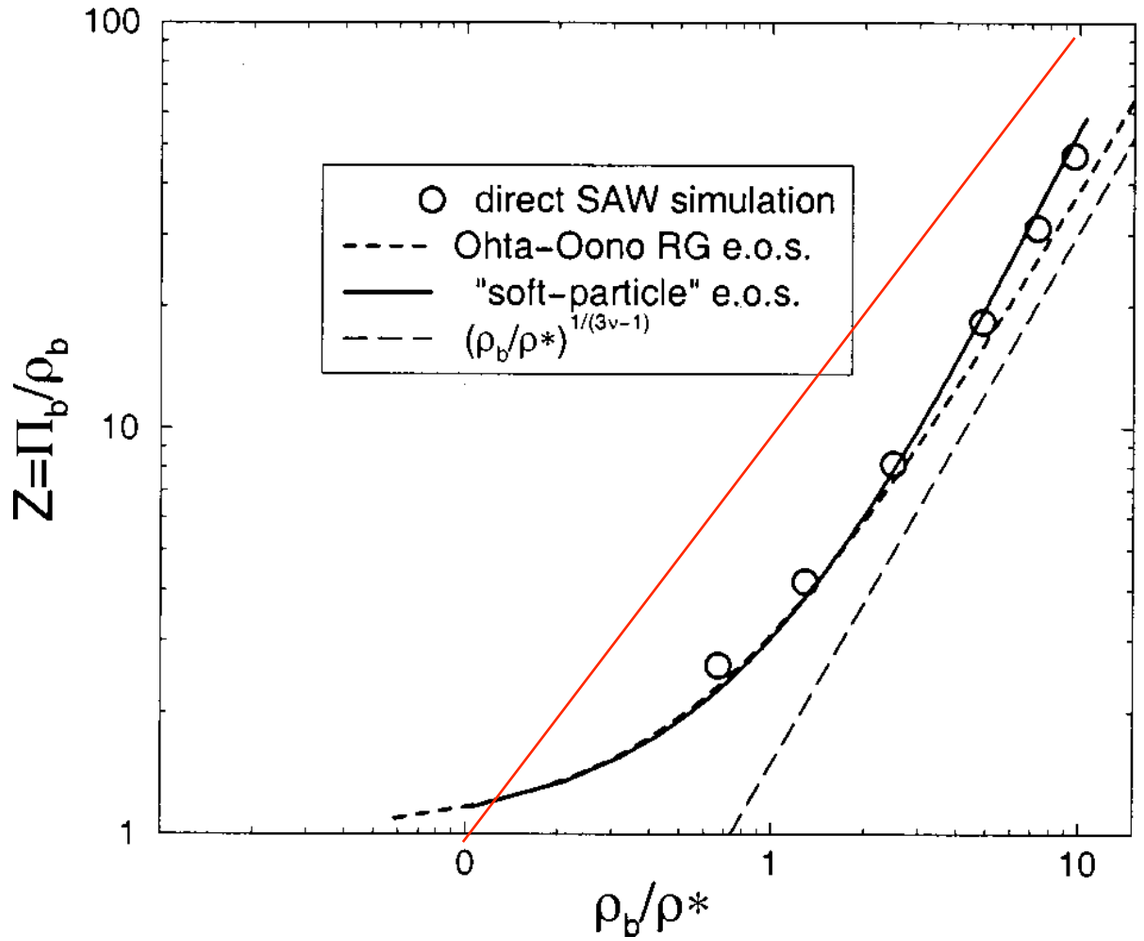

FIG. 11. Log–log plot of the e.o.s. $Z = \Pi/\rho_b$ as a function of the density for $L = 500$ polymers. The soft-particle e.o.s. gives a good representation of the full SAW polymer simulations. At the highest densities there is a slight deviation from the expected des Cloizeaux $(\rho_b/\rho^*)^{1/(3\nu-1)}$ scaling law which we attribute to the effects of a finite monomer concentration c. Also shown is the RG e.o.s. of Ohta and Oono (Refs. 60, 61).

Coarse-grained model for polymer solutions

Same strategy to compute hard wall-polymer effective interactions

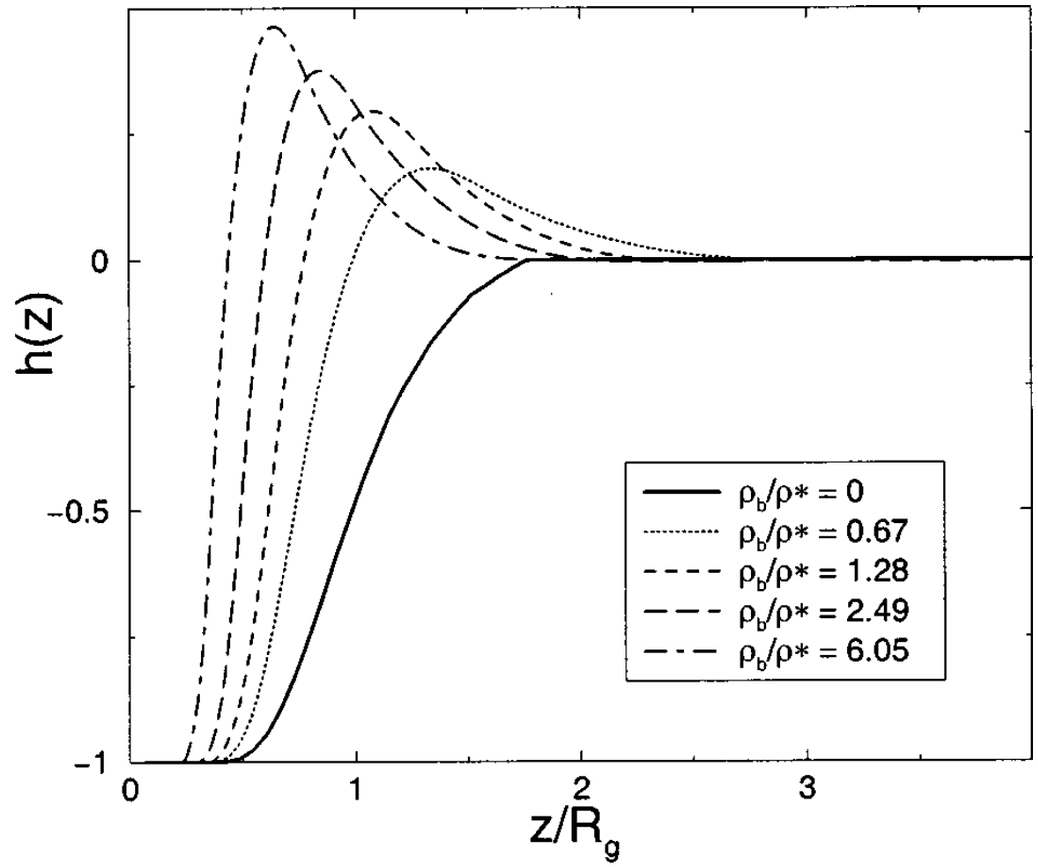

FIG. 13. The wall–polymer CM density profile $h(z)=\rho(z)/\rho_b-1$ for SAW polymers at different bulk concentrations. From $h(z)$ we can calculate the corresponding polymer absorptions Γ and find $-\Gamma=0$, 0.094, 0.13, 0.16, and 0.20 in units of R_g^{-2}, respectively. The relative absorptions are $-\Gamma/\rho_b=0.84$, 0.59, 0.41, 0.27, and 0.14 R_g, respectively, and decrease with increasing density as expected.

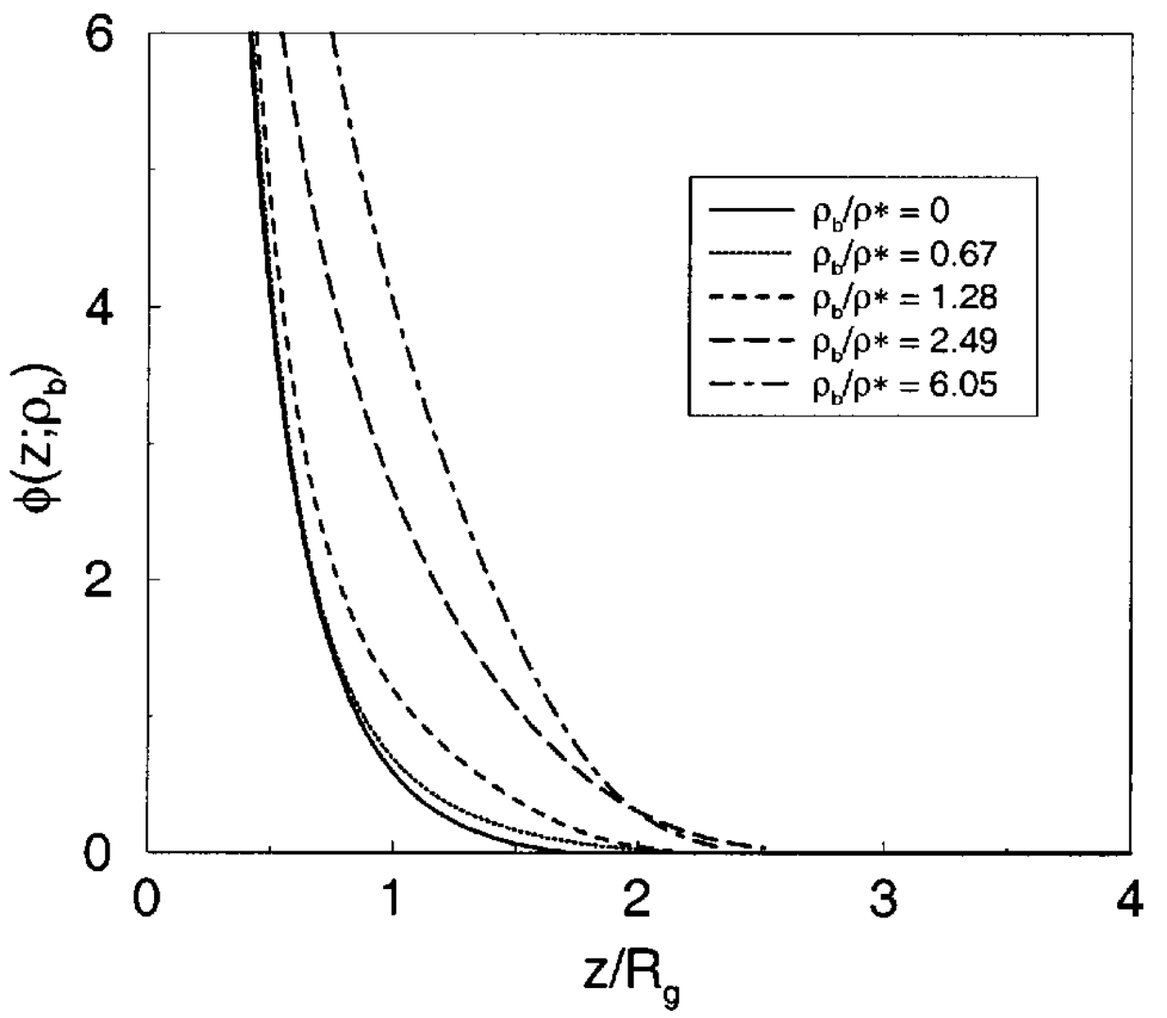

FIG. 15. The wall–polymer potential $\phi(z;\rho_b)$ as obtained from the inversion of $h(z)$ via the HNC expression, Eq. (20).

Coarse-grained model for polymer solutions

Depletion potential:
the interaction free energy per unit area can be obtained by integrating the osmotic pressure

$$\Delta F(d)/A = \int_d^\infty dz(\Pi(z) - \Pi(\infty)),$$

excellent agreement between effective and full monomer simulations

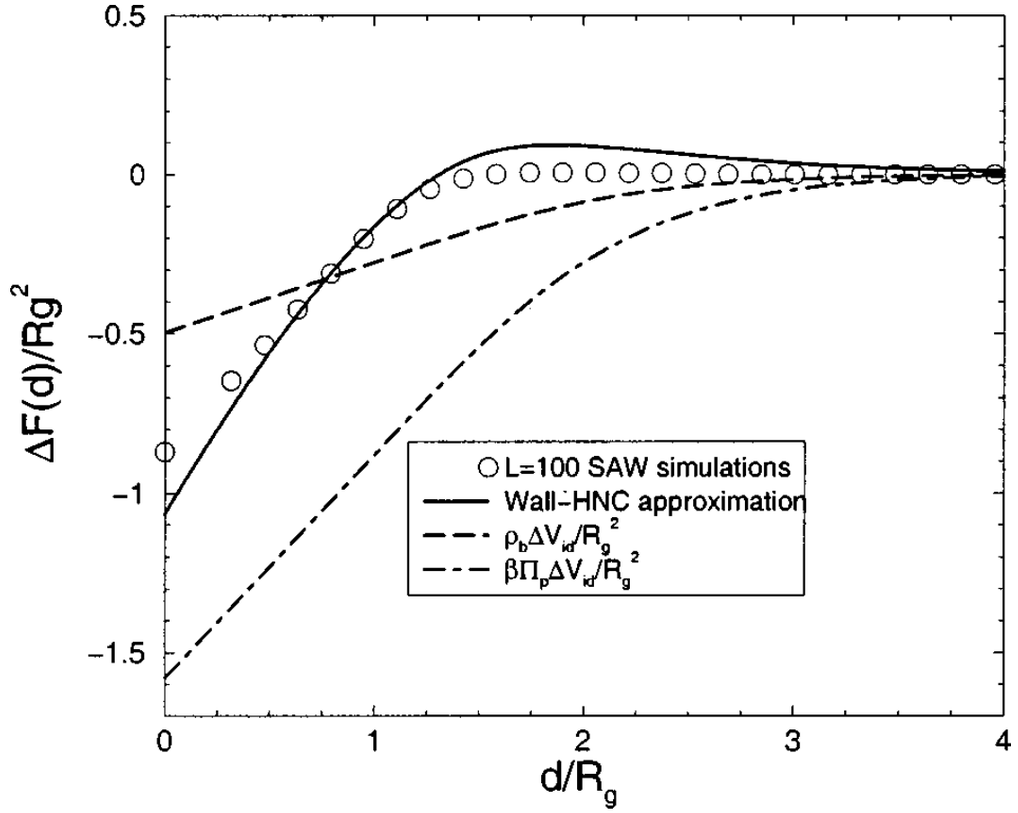

FIG. 21. Depletion free-energy $\Delta F(d)/R_g^2$ between two plates separated by d for $\rho_b/\rho^* = 0.95$. Circles are the ''exact'' MC simulations of SAW polymers. The long-dashed and dashed–dotted lines denote the two AO approximations mentioned in the text. The short-dashed line denotes the more accurate wall-HNC approximation of Eq. (24), which is, in fact, very close to the simulations in the soft particle picture shown in Fig. 18.

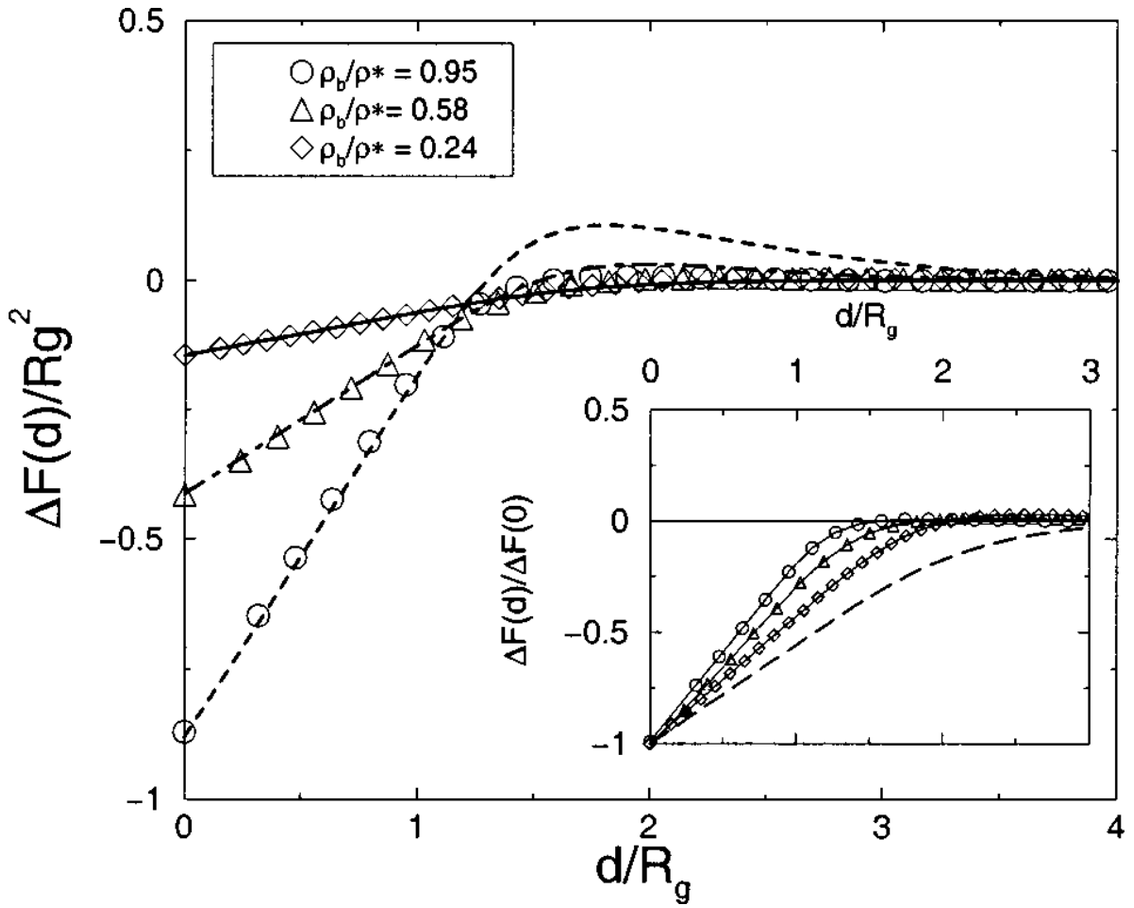

FIG. 18. Depletion free-energy $\Delta F(d)/R_g^2$ between two plates separated by d, for three densities, $\rho_b/\rho^* = 0.95$, $\rho_b/\rho^* = 0.58$, $\rho_b/\rho^* = 0.24$. The symbols denote the ''exact'' MC simulations, while the dashed, dashed–dotted, and solid lines are the soft-colloid simulations for the same densities. (Inset) $\Delta F(d)/\Delta F(0)$ for the SAW simulations, the solid lines are to guide the eye. The long-dashed line is the ideal Gaussian polymer result calculated in the Appendix. Note that the range decreases with density, and that, even for the lowest density, the AO ideal polymer approximation overestimates the interaction range.

Star polymers in good solvent

Star polymers consist of **f** linear polymer chains chemically anchored to a common centre. Typical values of **f** can go from **f=1** (linear chain) to **f~500**.

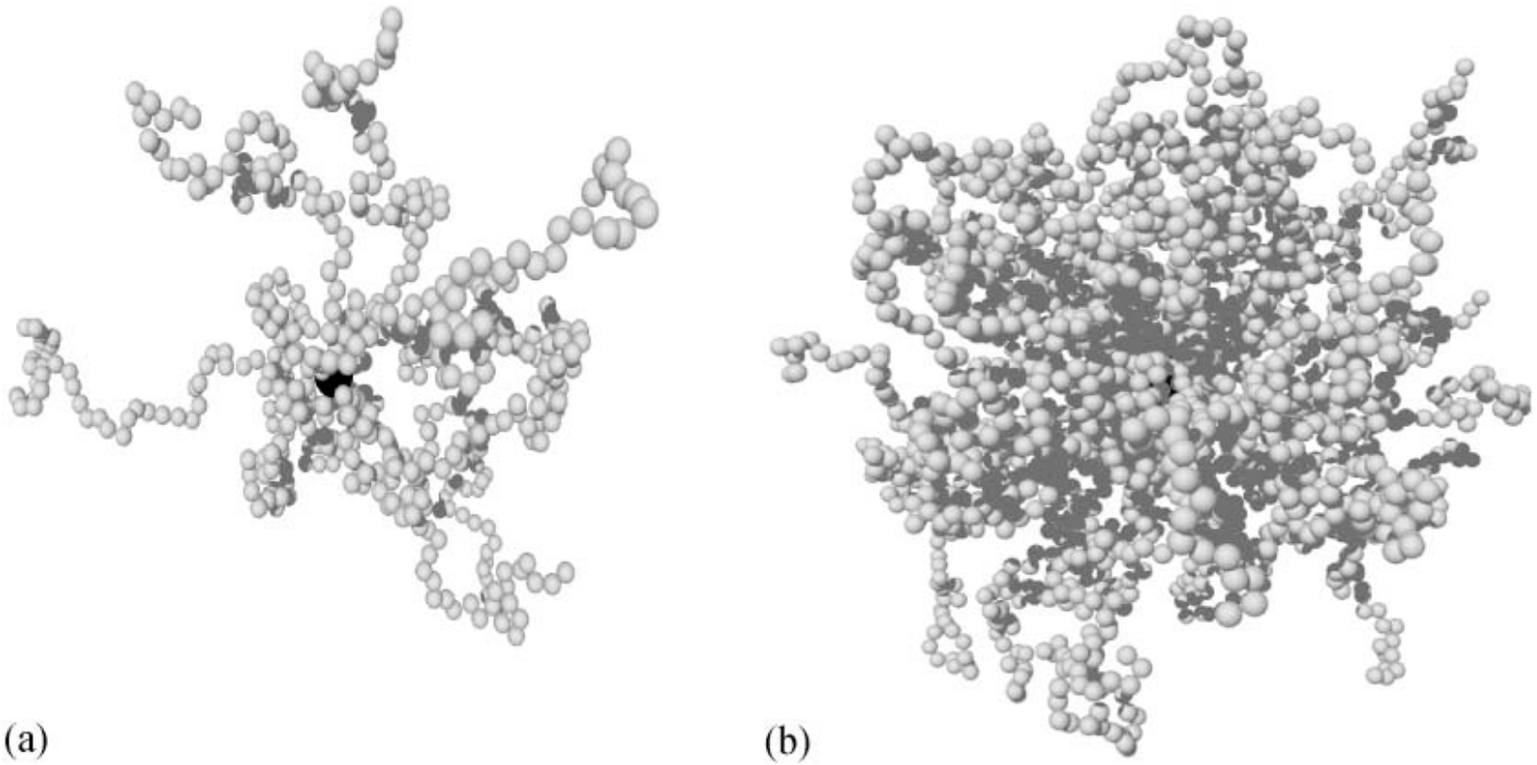

Fig. 37. Snapshots of star polymers in good solvents as obtained from MD simulations employing the model of Grest et al. [330] with: (a) $f = 10$, $N = 50$, and (b) $f = 50$, $N = 50$. For small f, the star looks like a fractal, aspherical object whereas for large f it resembles a spherical, colloidal particle. (Taken from Ref. [331].)

- Small **f**: the star looks like a fractal object
- Large **f**: the star looks more compact like a colloidal particle

- Full monomer simulation of many starts in a wide range of **f** is out of reach.
- Full monomer simulation of two stars to extract the zero density two body effective potential and use in in many stars effective simulation.

Interaction between two stars

Direct simulation of two stars for many vaules of **f**

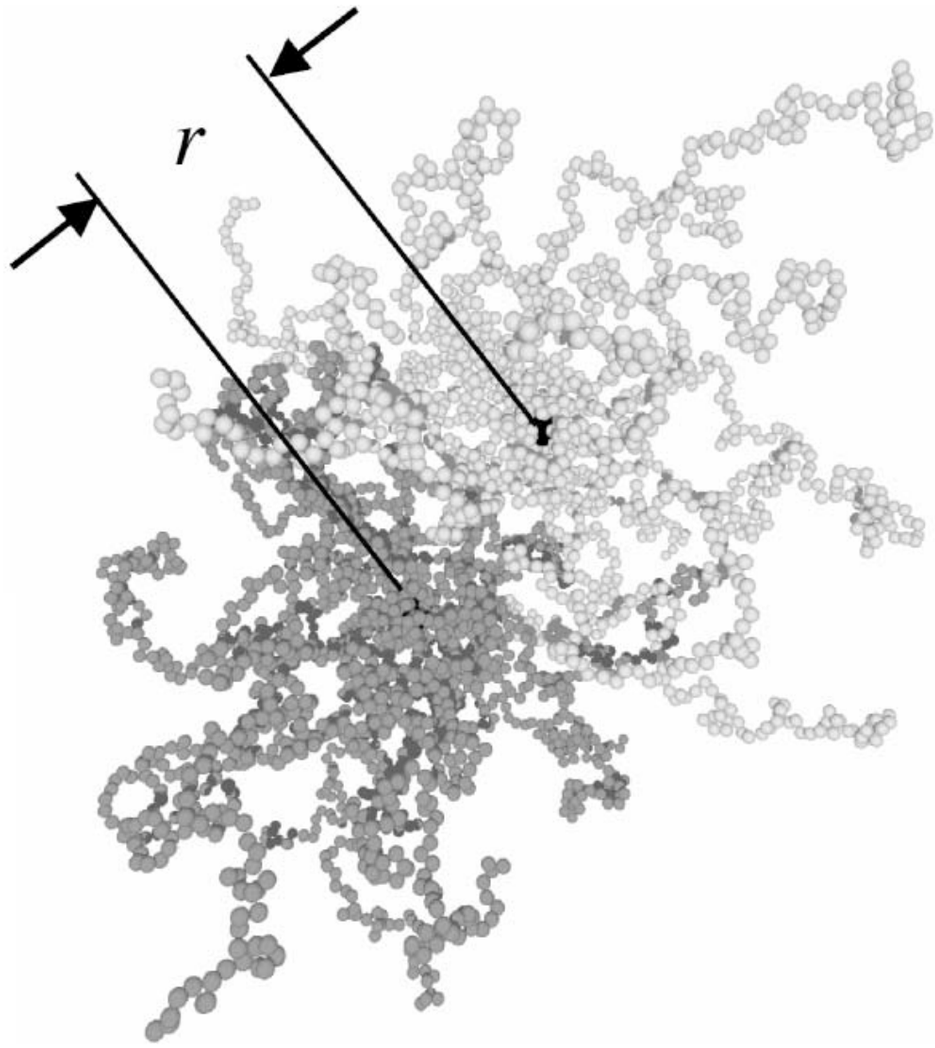

•Small **f** (≤10): log-Gauss potential

$$v(r) = \frac{5}{18} k_{\rm B} T f^{3/2} \begin{cases} -\ln(\frac{r}{\sigma}) + \frac{1}{2\tau^2\sigma^2} & \text{for } r \le \sigma; \\ \frac{1}{2\tau^2\sigma^2} \exp\left(-\tau^2 \frac{r^2-\sigma^2}{\sigma^2}\right) & \text{for } r > \sigma, \end{cases}$$

• Large **f** (>10): log-Yukawa potential

$$v(r) = \frac{5}{18} k_B T f^{3/2} \begin{cases} -\ln(\frac{r}{\sigma}) + \frac{1}{1+\sqrt{f}/2} & \text{for } r \le \sigma \\ \frac{\sigma}{1+\sqrt{f}/2} \frac{\exp(-\sqrt{f}(r-\sigma)/2\sigma)}{r} & \text{for } r > \sigma \end{cases}$$

σ is the size of the corona: $\sigma = 1.26 R_g$

Three stars interaction is negligible small outside the corona and ~10% of the energy for penetrating coronae.

Two body interaction is adeguate for many stars systems provided the number density of stars is not much higher than the overlapping density $\rho^* = 1/\sigma^3$.

Phase Diagram of Star Polymer Solutions

M. Watzlawek,[1,*] C. N. Likos,[1,2] and H. Löwen[1,2]

packing fraction:

$$\eta = \frac{\pi}{6}\rho\sigma^3$$

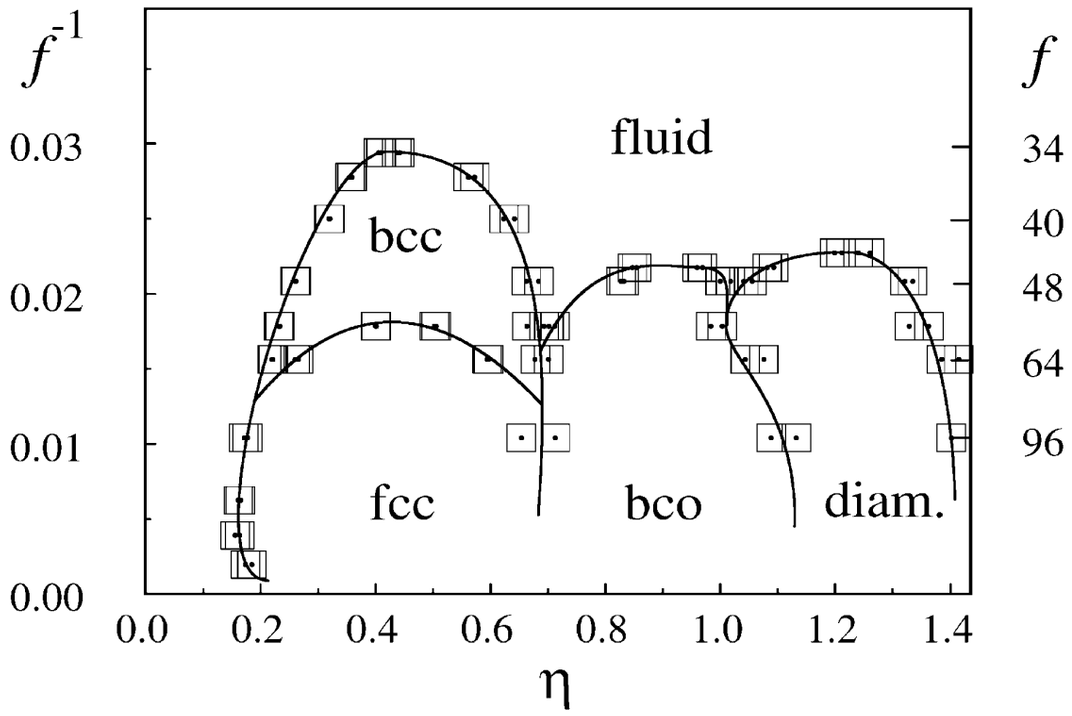

Fig. 48. The phase diagram of star polymer solutions in a good solvent, as obtained from the simulations, drawn on the (η, f)-plane. The squares indicate the phase boundaries. The lines, drawn as a guide to the eye, should in principle be double but the density gaps between coexisting phases are so narrow that this would only crowd the figure without adding significant information. (Taken from Ref. [319].)

- f<34: no stable crystal phase
- 34<f<50: fluid-bcc-fluid reentrant phase diagram for increasing packing
- f>50: the fluid is only stable at very low packing
- 0.2<η<0.7: bcc to fcc transition for increasing f
- η>0.7, f>50: highly anisotropic crystal structures are favoured even with a sperically symmetric pair potential